

# Secondary Stability Assessment of Titanium Implants with an Alkali-Etched Surface: A Resonance Frequency Analysis Study in Beagle Dogs

Jakub Strnad, MSc, PhD<sup>1</sup>/Karel Urban, Dr Med, PhD<sup>2</sup>/  
Tibor Povysil, Dr Med, Dr Sc Prof<sup>3</sup>/Zdenek Strnad, MSc, PhD<sup>4</sup>

**Purpose:** This study was carried out to quantify the effect of an alkali-modified surface on implant stability during healing using an animal model. **Materials and Methods:** A total of 24 screw-shaped, self-tapping, commercially pure titanium dental implants, divided into a test group (implants with an alkali-modified surface or "biosurface") and a control group (implants with a turned, machined surface) were inserted without pretapping in the tibiae of 3 beagle dogs. The resonance frequency analysis method was used to measure the implant stability quotient (ISQ) 0, 1, 3, 9, and 12 weeks after implantation. The animals were sacrificed after 2, 5, and 12 weeks, and the bone-implant contact (BIC%) was evaluated histomorphometrically. **Results:** The difference in the osseointegration rates ( $\Delta$ ISQ/ $\Delta$ healing time) between the implants with alkali-modified surface (biosurface) and those with a turned, machined surface was evaluated as a mean of 0.843 ISQ/week within the first 9 weeks of healing. The mean increase in the secondary implant stability was found to be proportional to the mean increase in the BIC at healing period earlier than 5 weeks. **Discussion:** The characteristics that differed between the implant surfaces, ie, specific surface area, contact angle, and hydroxylation/hydration, may represent factors that influence the rate of osseointegration and the secondary implant stability. **Conclusion:** The alkali-treated surface enhances the secondary stability in the early stages of healing compared to the turned, machined surface, as a consequence of faster BIC formation. INT J ORAL MAXILLOFAC IMPLANTS 2008;23:502-512

**Key words:** alkali-etched surface, bioactive surface, dental implants, histometric analysis, resonance frequency analysis, secondary stability

In modern dental implantology, advanced treatment protocols (eg, early or immediate loading) are frequently used to reduce treatment time. Shortening the

healing period entails new demands on both the primary and secondary stability of the implant. Primary implant stability is mainly dependent on the mechanical characteristics of the original bone (its local quality and quantity), the type of implant used (its geometry, diameter, length, and surface), and the surgical techniques employed. Secondary stability represents enhancement of the stability as a result of peri-implant bone formation through gradual bone remodeling and osteoconduction, with the possibility of new bone formation at the implant-bone interface.<sup>1</sup> Contemporary knowledge indicates that the degree of micromotion at the bone-implant interface (primary stability) during initial healing is of utmost importance in achieving good secondary stability.<sup>2-4</sup> However, several experimental and clinical studies have shown that secondary stability is also strongly influenced by the implant surface characteristics.<sup>5,6</sup>

<sup>1</sup>Chief Scientific Officer, Laboratory for Glass and Ceramics, Lasak, Prague, Czech Republic.

<sup>2</sup>Associate Professor, Orthopedic Clinic, Teaching Hospital, Charles University, Hradec Králové, Czech Republic.

<sup>3</sup>Professor, Institute of Pathology, 1st Medical Faculty of Charles University and Institute for Postgraduate Studies, Prague, Czech Republic.

<sup>4</sup>Associate Professor, Laboratory for Glass and Ceramics, Lasak, Prague, Czech Republic.

**Correspondence to:** Dr Jakub Strnad, Laboratory for Glass and Ceramics, Lasak, Papirenska 25, Prague 16000, Czech Republic. Fax: +420 224 319 716. E-mail: strnad@lasak.cz

To enhance secondary stability and accelerate the formation of stable and functional bone-implant interfaces, a number of implant surfaces have been developed. Surface roughness is the most frequently studied property affecting secondary stability. A summary of a number of studies<sup>7,8</sup> providing analysis of bone-implant contact and removal torque values using animal models, indicates that roughened titanium surfaces generally exhibit greater contact with the bone and/or higher removal torque values than smoother implant surfaces, such as turned, machined or polished titanium surfaces. Some authors suggested that surfaces with mean roughness of 1.0 to 1.5  $\mu\text{m}$  exhibit stronger bone response than smoother or rougher implant surfaces.<sup>9–12</sup> These suggestions do not take into consideration chemical composition changes and physical chemical property variations introduced to the compared surfaces by the roughening procedures. It has been shown that the optimal roughness value varies according to the chemical composition and physical chemical properties of the tested surfaces and that, in some cases, the bone response can be more strongly affected by these parameters than by the roughness alone.<sup>13–15</sup>

Currently, surface modification of titanium by acid etching of turned or sandblasted titanium surfaces to create a micro-rough texture is being introduced to support and accelerate the healing and bone formation processes around the implant.<sup>16–21</sup> Some experimental studies have indicated that acid-etched surfaces with minimal roughness ( $R_a = 0.62 \mu\text{m}$ )<sup>16</sup> or greater roughness ( $R_a = 2.15 \mu\text{m}$ )<sup>17</sup> exhibit a stronger bone response compared to sandblasted, moderately rough surfaces ( $R_a = 1.26 \mu\text{m}$ )<sup>16</sup> or to mechanically turned, machined low-roughness surfaces ( $R_a = 0.86 \mu\text{m}$ ).<sup>17</sup> Some acid-etched implants with a micro-rough texture can accelerate the osseointegration processes despite their minimal roughness compared to the moderately roughened sand-blasted surfaces.

The surface chemistry of titanium implants is also thought to affect the secondary stability independently of the surface topography although it is difficult to separate the effects of these 2 factors. There is extensive experimental evidence in the literature showing that biomaterials with different chemical compositions trigger different biologic responses.<sup>22–26</sup> A specific biologic response is elicited at the interface with bioactive materials with high surface reactivities,<sup>14</sup> resulting in the formation of a bond between the tissue and the material surface.<sup>22</sup> Bioactive materials with special chemical compositions, including bioactive glasses, bioactive glass ceramics, hydrated silica, and titanium gel oxides or hydroxyapatite have the ability to very rapidly form a stable interface with bone tissue following the formation of calcium phos-

phate deposition on their surfaces as a consequence of chemical interaction with body fluids.<sup>22</sup> For instance, 50% bone-implant contact is achieved within 7 days for bioactive glasses.<sup>22</sup> The mechanical strength of this interface usually exceeds the strength of the bone tissue to which the bioactive material is bonded.<sup>27,28</sup> However, because their poor mechanical properties prevent their use as solid implants under high load-bearing conditions, bioactive materials (especially hydroxyapatite) are generally used as a coating applied on the surface of titanium implants to achieve faster and more reliable bonding with bone tissue. In spite of the success achieved in accelerating the bone healing process and in exhibiting greater tolerance to low primary stability in the early phases of healing,<sup>21–31</sup> hydroxyapatite plasma-sprayed coatings have often been the subject of controversy regarding their stability<sup>32,33</sup> and low long-term success rate.<sup>34,35</sup> On the other hand, some medium-term and long-term clinical studies demonstrate the high success rate of hydroxyapatite-coated implants.<sup>36–38</sup> The literature tends to indicate the imperfect adhesion of the hydroxyapatite surface layers and their chemical and mechanical instability rather than their inability to substantially improve osseointegration, especially in the initial stages of healing.

Various attempts have been made to modify the titanium surface to make it bioactive without the use of a thick coating of another bioactive material. The most successful methods of titanium bioactivation have been, for example, alkali or fluoride treatment.<sup>39–41</sup> Recently, an alkali-modified surface for titanium dental and spinal implants was clinically introduced under the brand name Bio-surface as a potentially bioactive surface.<sup>42–47</sup> The present study was carried out to quantify the effect of this surface modification on the implant stability during healing, using resonance frequency analysis and histologic examination on an animal model. This study also describes the characteristic surface properties of this surface and compares them with the turned, machined titanium surface.

## MATERIALS AND METHODS

### Implant Materials

A total of 24 screw-shaped, self-tapping, (c.p.) titanium dental implants divided into a control group (12 implants with a turned, machined surface) and a test group (12 implants [Lasak, Prague, Czech Republic]) with sandblasted, acid-, and alkali-treated surface [Biosurface; Lasak]) were inserted without pretapping into the tibiae of 3 beagle dogs. Identically shaped implants with a diameter of 3.7 mm and a length of 10 mm were used for the test and control groups.

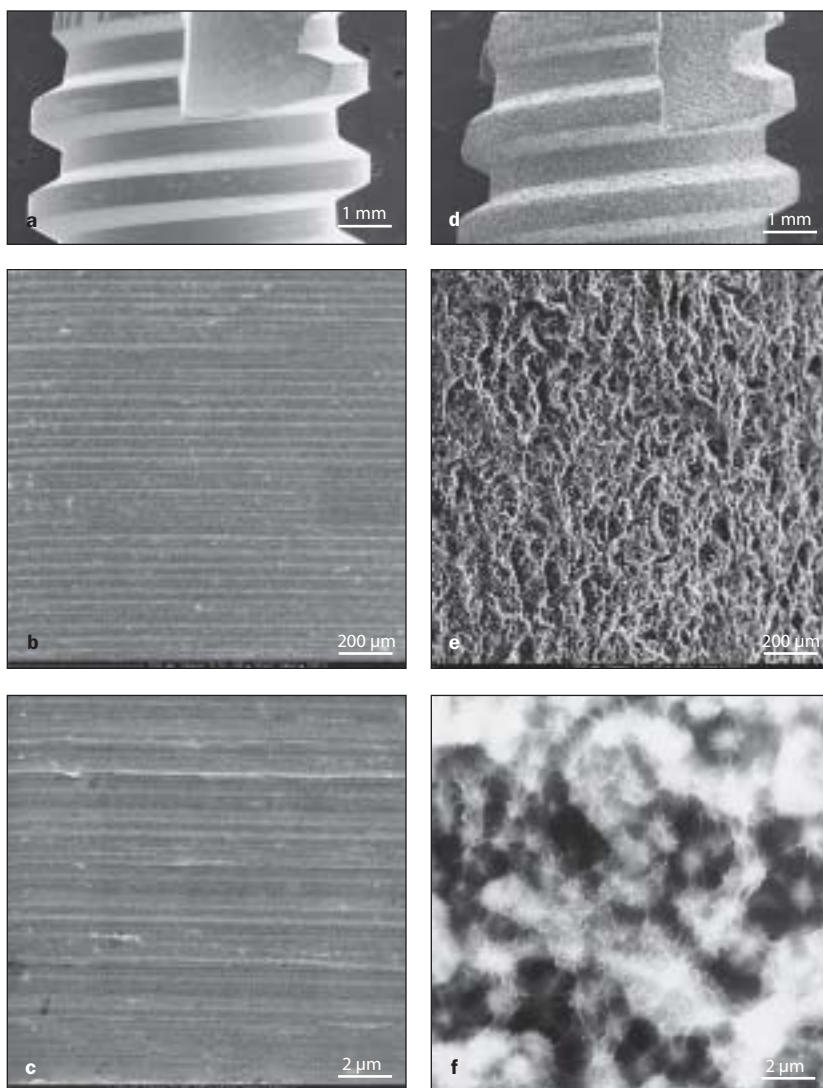


**Fig 1** SEM images of (a to c) the turned, machined surface and (d to f) the biosurface (original magnification a and d  $\times 30$ ; b and e  $\times 200$ , c  $\times 1500$ ; f  $\times 4000$ ).

### Surface Characterization

The overall surface morphology of the employed implants was characterized using a scanning electron microscope (SEM, Hitachi, Tokyo, Japan) with an accelerating voltage of 15 to 30 kV (Fig 1). Surface roughness measurement was carried out using a scanning surface topography instrument, a Talysurf CLI 1000 with a confocal CLA gauge (Taylor Hobson, Leicester, United Kingdom), which provides highly accurate non-contact 3-dimensional measurements. The following were measured for 3 implants in each group: 3 thread tops, 3 thread valleys, and 3 thread flanks. Four 3-dimensional parameters (amplitude, spacing, and hybrid) were calculated (Table 1). The original unfiltered measurements and measurements made with a filter size of  $50 \times 50 \mu\text{m}$  were evaluated.

Dynamic contact angle measurement was performed by the Wilhelmy plate method using a Tensiometer K15 instrument (Kruss, Hamburg, Germany).

The wetting angle values in water were determined from the dependence of the wetting force on the immersion depth. The mean values of the wetting angle were calculated from 4 repeated measurements (Table 2). The specific surface area was determined by the BET krypton gas adsorption method. The surface area is expressed in relation to unit geometric surface area of the implant as the mean value of 4 repeated measurements (Table 2). The determination was performed using an ASAP 2010 M instrument (Micromeritics, Norcross, GA). Diffuse reflectance infrared Fourier transform (DRIFT) spectroscopy was used to determine the degree of surface hydration. The measurement was performed on a Nicolet 740 instrument (Nicolet, Madison, WI). Hydroxyl group density was expressed as the radiation absorption in Kubelka-Munk units (KMU) evaluating a band at  $3,400 \text{ cm}^{-1}$  with resolution of  $4 \text{ cm}^{-1}$  (Fig 2).

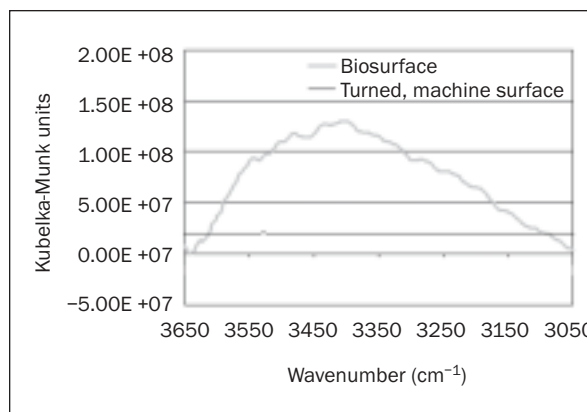
**Table 1 Mean Roughness Parameters of Bio- and Turned, Machined Implant Surfaces Measured at 3 Different Sites of Implant Threads**

Surface treatment/ Sites of measurement	Sa ( $\mu\text{m}$ )		Sq ( $\mu\text{m}$ )		Sdr (SD) (%)		Sds ( $\mu\text{m}^2$ )	
	Mean	SD	Mean	SD	Mean	SD	Mean	SD
Gaussian filter size $50 \times 50 \mu\text{m}$ (roughness)								
Biosurface								
Top	1.11	0.13	1.50	0.19	15.90	4.50	0.019	0.002
Valley	1.32	0.27	1.72	0.36	18.28	7.46	0.022	0.003
Flank	1.15	0.14	1.55	0.20	19.99	6.88	0.031	0.003
Machined								
Top	0.57	0.14	0.73	0.17	8.35	3.06	0.025	0.005
Valley	0.28	0.03	0.36	0.03	2.50	0.04	0.051	0.009
Flank	0.50	0.11	0.68	0.18	8.29	4.10	0.034	0.004
Original unfiltered measurement								
Biosurface								
Top	2.41	0.23	3.17	0.33	24.28	7.39	0.049	0.009
Valley	2.47	0.50	3.15	0.64	29.05	12.13	0.065	0.010
Flank	2.41	0.34	3.11	0.47	37.91	15.90	0.103	0.019
Machined								
Top	0.65	0.14	0.82	0.18	11.41	3.67	0.057	0.013
Valley	0.50	0.06	0.62	0.07	4.22	0.41	0.115	0.019
Flank	0.86	0.30	1.10	0.35	13.24	5.90	0.082	0.018

Sa = arithmetic average height deviation; Sq = root mean square of height deviation; Sdr = developed surface ratio, Sds = the number of summits in a unit sampling area.

**Table 2 Contact Angles and Specific Surface Areas of Biosurfaced Implants and Machined Implants**

Surface treatment	Contact angle		Specific surface area Mean $\pm$ SD ( $\text{mm}^2/\text{mm}^2$ )	
	Mean	SD	Mean	SD
Biosurface	27.2	6.9	138.0	42.5
Turned, machined surface	79.5	4.6	1.4	0.7

**Fig 2** DRIFT spectra of turned, machined surfaces, and biosurfaces.

### Surgical Procedure and Implant Placement

Three beagle dogs (mean weight,  $16 \pm 2$  kg; mean age, 2 years) were used in this study, which was approved by the Ethics Committee for Work with Experimental Animals at the Teaching Hospital, Charles University, Hradec Králové, Czech Republic. Anesthesia was carried out using a dose of 15 mg/kg of 5% Narkamon (Spofa, Prague, Czech Republic) and 2 mg/kg of 2% Rometar (Spofa). The animals were pre-medicated with a dose of 0.05 mg of Atropin (Biotica, Slovenská Lupca, Slovakia) 30 minutes prior to surgery. Under total anesthesia, in a supine position, following the usual preparation of the operation field and towelings, a surgical cut with a length of approximately 7 cm was made on the anteromedial surface of the tibia. A sharp cut was made in the fascia and then in the periosteum, which was widened to the

side with a raspator. Following uncovering of the surface of the tibia, the positions for drilling the holes for implanting the tested implants were marked. The implant sites were prepared with 1.5-mm, 2.0-mm pilot, and 3.0-mm drills at 800 rpm with simultaneous cooling with a physiologic solution. A countersink drill was then used. The implants were screwed in with an insertion torque of approximately 40 Ncm. The biosurfaced and machined implants were alternately inserted in the tibia side by side (eg, biosurfaced, machined, biosurfaced, and so on), as depicted in Fig 3. The order of the implants was the opposite in the other leg of the same animal (eg, machined, biosurfaced, machined, and so on). The first animal received 12 implants (6 from each group). Each of the other 2 animals received 6 implants (3 from each group). In the first animal, implantation was followed by measur-

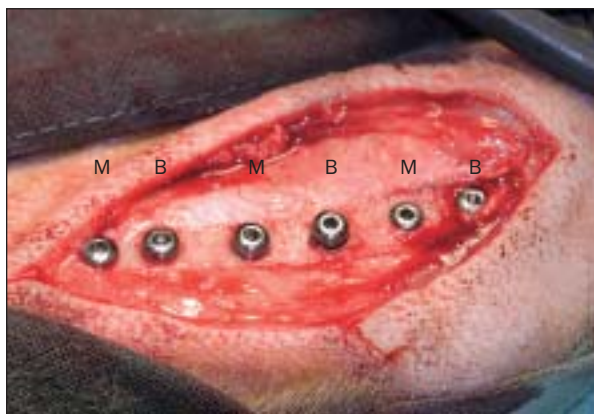


**Fig 3** The order in which the implants were placed from the medial aspect of the tibia on down (left leg). B = biosurface, M = machined surface.

ing the stability of the implants using resonance frequency analysis. A probe was screwed into the cervical part of the implant, and the soft tissues were pulled to one side with a hook so that they did not affect the probe. The measurement was carried out twice for each implant. This was followed by rinsing of the operation incision. The implants were closed with cover screws, and, following control of hemostasis, the operation incisions were closed in layers and were finally covered with a sterile bandage. Implant stability measurement was repeated for each implant in the 1st, 3rd, 9th, and 12th weeks using the same procedure. Following completion of the experiment, the dogs were sacrificed after 2, 5, and 12 weeks by an overdose of thiopental (ICN, Roztoky u Prahy, Czech Republic), and the tibiae were removed and fixed in 10% formaldehyde prior to histologic evaluation.

### Implant Stability Measurement

The resonance frequency analysis (RFA) method was used to measure implant stability. The measurement was performed using an Osstell instrument (Integration Diagnostics, Göteborg, Sweden) with a commercially available transducer (type F37 L5). The perpendicular orientation of the transducer along the long axis of the bone was always maintained. The transducer, which is fixed to the implant in the bone, contains a wave source and an analyzer. The wave source vibrates with gradually increasing frequency. The analyzer records the frequency of the source, causing the resonance in the transducer-implant-bone system, including the bone-implant interface. The recorded frequency value in Hz is converted to an implant stability quotient (ISQ) value, which varies in a range from 0 to 100, with 100 indicating maximum stability. The method allows measurement with a precision of  $\pm 1$  ISQ.

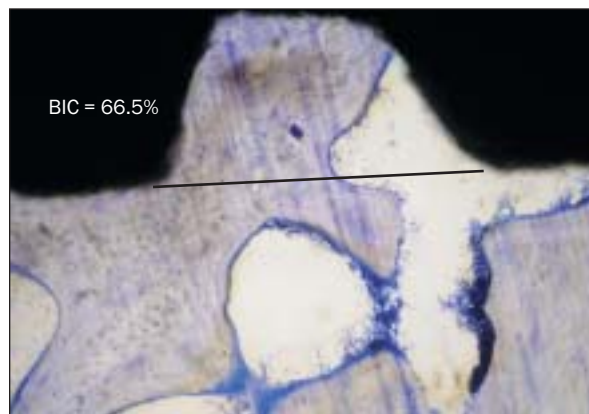


**Fig 4** Histometric analysis. Evaluation of the bone-implant contact (%BIC).

### Histologic Preparation and Analysis

The tibiae were dissected and blocks of 7 mm thickness containing 1 implant each were prepared. Non-decalcified (ground) sections were processed according to the method of Donath and Breuner.<sup>48</sup> Thin sections with a thickness of 30 to 50  $\mu$ m were stained with toluidine blue and examined using an optical microscope (Olympus BX-60, Tokyo, Japan) equipped with an image system (Quick PHOTO Industrial 2.0; Olympus, Prague, Czech Republic). Bone-implant interfaces at the threaded part were histometrically analyzed by evaluating the percentage of bone-implant contact (BIC). The length of the bone tissue in direct contact with the implant (BC) and the total interface length (IL) were measured (Fig 4). The percentage of BIC is given by the ratio of the direct contact length to the total interface length multiplied by 100. The presented mean values were calculated from the 3 sections as an average for each implant for both types of implant surface.

### Statistical Analysis

Implant stability quotient (ISQ) and BIC% data are reported as mean values with standard deviations (SD).

Nonparametric Friedman's analysis of variance (ANOVA) was performed to analyze variations of ISQ and BIC% during the 12-week follow-up period. The analysis was followed by nonparametric Wilcoxon tests to determine differences within groups between particular time intervals. To investigate the statistical significance of the implant group differences, the data were subjected to the nonparametric Mann-Whitney tests. A difference was considered significant when  $P < .05$ .

To determine the difference in the osseointegration rate between the test and control groups, the time-dependence of the differences (test ISQ – control ISQ and test BIC% – control BIC%) were evalu-

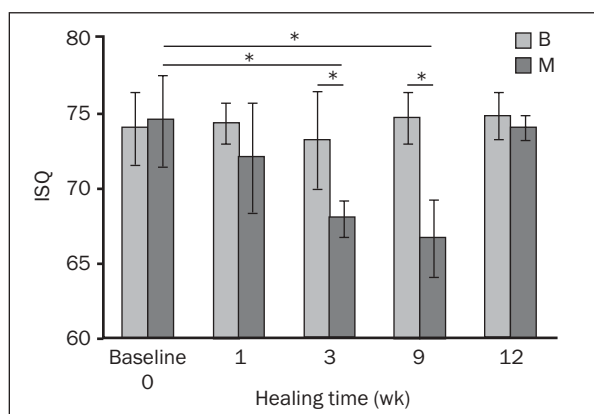


**Fig 5** Mean implant stability (ISQ ± SD) of biosurfaced implants (B) and machined implants (M) at placement (baseline) and after 1, 3, 9, and 12 weeks. \* indicates significant difference ( $P < .05$ ).

ated by the method of linear regressions and the parameters of the straight lines (slopes and intercepts) were determined. These parameters were calculated together with the  $P$  values, reliability limits, and correlation coefficients. The values of the physico-chemical properties of surfaces are presented as mean values and standard deviations (SD).

## RESULTS

### Primary Implant Stability and Variation of Implant Stability During Healing

The mean ISQs for the machined and biosurfaced groups ( $\pm$  SD) at baseline (primary stability) and at 1, 3, 9, and 12 weeks are presented in Fig 5.

The RFA measurements indicate similar mean primary stabilities for both groups of monitored implants ( $74.0 \pm 2.45$  for biosurfaced and  $74.5 \pm 2.99$  for machined); no significant difference was observed between the 2 groups ( $P = .871$ ; Mann-Whitney test). Friedman ANOVA revealed no statistically significant differences in biosurface-group ISQ at any of the measured time points ( $P = 0.482$ ). In contrast, significant differences ( $P < .001$ ) were revealed during the 12-week follow-up for the machined group. There was a statistically significant decrease in ISQ between baseline and 3 ( $P = .028$ ) and 9 ( $P = .028$ ) weeks (Wilcoxon matched pairs test). A statistically significant difference between the test and control groups was observed after 3 ( $P = .0035$ ) and 9 ( $P = .0035$ ) weeks (Mann-Whitney test; Fig 5).

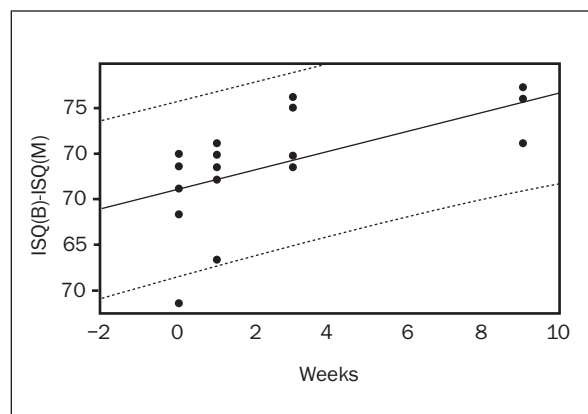


**Fig 6** Time dependence of implant stability difference (biosurface ISQ - machined ISQ). Regression straight line: biosurface ISQ - machined ISQ =  $0.843 \times \text{time (weeks)} + 1.0111$ . Boundaries of reliability are shown (dashed lines). Correlation coefficient  $r = 0.756$ .

The time dependence of the differences (biosurface ISQ - machined ISQ) in the first 9 weeks of follow-up was evaluated by the method of linear regressions, and the parameters of the straight line (slope and intercept) were determined as follows: biosurface ISQ - machined ISQ =  $0.843 \times \text{time (weeks)} + 1.0111$  (Fig 6). The correlation coefficient ( $r = 0.6561$ ) indicated a moderately strong relationship between variables; the slope of the regression line was positive and statistically significant ( $P < .001$ ).

### Histologic Examination (Histologic Observations)

Histologic examination of the bone-implant interface was performed for both types of tested implant surfaces 2, 5, and 12 weeks after implantation. Three implants from each group were evaluated for each time interval. The cervical part of the implants was mostly surrounded by cortical bone, while the thread part was surrounded by trabecular bone. Close BIC was frequently observed at the cervical part of the implants with the biosurface. In contrast, the specimens with turned, machined surfaces showed patchy BIC, and intermediate soft tissue was indicated in some cases (Fig 7). The time development of the bone-implant contact (BIC%) at the thread part of the implant was evaluated histometrically (Figs 8 and 9). The results of the histometric analysis are presented in Fig 10.

Friedman ANOVA revealed statistically significant differences in BIC% for the test group ( $P = .029$ ) as well as the control group ( $P = .032$ ) at all measured

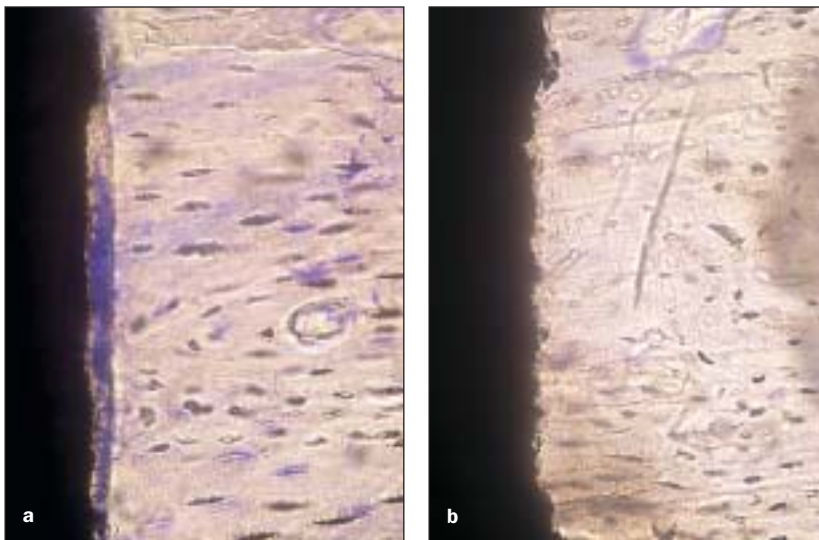


**Fig 7** Photomicrographs of the bone-implant interface at the cervical part of the implants with (a) a machined surface and (b) a biosurface 2 weeks after implantation (toluidine blue; original magnification  $\times 500$ ). Histologic examination indicated the formation of intermediate soft tissue in the case of implants with machined surfaces.

time points. BIC of the biosurfaced group increased sharply during the first 2 weeks in contrast to the machined group, which exhibited a gradual increase starting at a later timepoint (Fig 11). Using the Mann-Whitney test, statistically significant differences between the test and control groups were observed after 2 weeks ( $P = .046$ ), 5 weeks ( $P = .049$ ), and 12 weeks ( $P = .049$ ).

The time dependence of the differences in BIC between the groups in the first 5 weeks was evaluated by the method of linear regressions, and the parameters of the straight line (slope and intercept) were determined as follows: test BIC – control BIC =  $7.94 * \text{time (weeks)} + 10.92$ . The positive slope of the regression line was found to have a correlation coefficient of  $r = 0.7561$  and to be statistically significant ( $P = .013$ ).

### Relationship Between Implant Stability and BIC

Evaluation of the correlation between the contribution of the biosurface to the implant stability (test ISQ – control ISQ) and the BIC (test BIC% – control BIC%) could not be performed by the standard method of correlation coefficients because of the experimental arrangement. Nevertheless, it was shown that test BIC% – control BIC% was proportional to time ( $P = .013$ ) as was test ISQ – control ISQ ( $P < .001$ ). This supports the hypothesis that during the first 5 weeks of the healing period, these 2 quantities are proportional to each other.

## DISCUSSION

This study presents the results of measurement of changes in the stability and BIC during healing of implants with biosurfaces and turned, machined surfaces.

RFA measurements showed that implants with machined surfaces exhibited a significant stability decrease after implantation. This decrease leveled off after as long as 12 weeks of healing. The biosurfaced implants did not show any significant stability change and maintained their stability during the monitored period. It was observed that even RFA indicated no change in implant stability with time (Fig 5); simultaneously, bone integration and increased bone-implant contact were observed (Fig 10). Similar results have been reported by several authors, showing that distinct BIC% may have similar values of implant stability or that implants with similar BIC% may have different ISQs. These results could be taken as an indication of lack of correlation between BIC and implant stability.<sup>49–52</sup> However, it must be borne in mind that the measured RFA data represent the total implant stability ( $ISQ_T$ ), which is composed of the contributions of the primary ( $ISQ_P$ ) and secondary ( $ISQ_S$ ) implant stability ( $ISQ_T = ISQ_P + ISQ_S$ ). Furthermore, when monitoring changes during healing, it must also be recalled that the contributions of these 2 factors (secondary and primary stability) change with the healing time. The secondary stability increases with increasing healing time as a result of new bone formation. The initial primary sta-

**Fig 8** Photomicrographs of the BIC at the threaded part of implants with (a) a machined surface and (b) a biosurface 5 weeks after implantation (toluidine blue; original magnification  $\times 200$ ). The BIC of the machined implant surface was a considerably lower value than the biosurface.

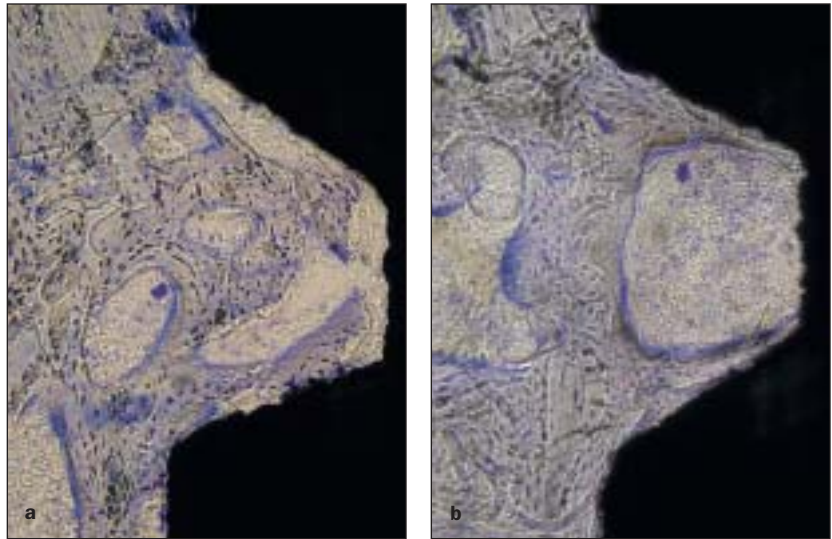


**Fig 9** Photomicrographs of the bone-implant interface at the threaded part of implants with (a) a machined surface and (b) a biosurface 12 weeks after implantation (toluidine blue; original magnification  $\times 200$ ). High BIC was seen in the threads of both the machined and biosurfaced groups.

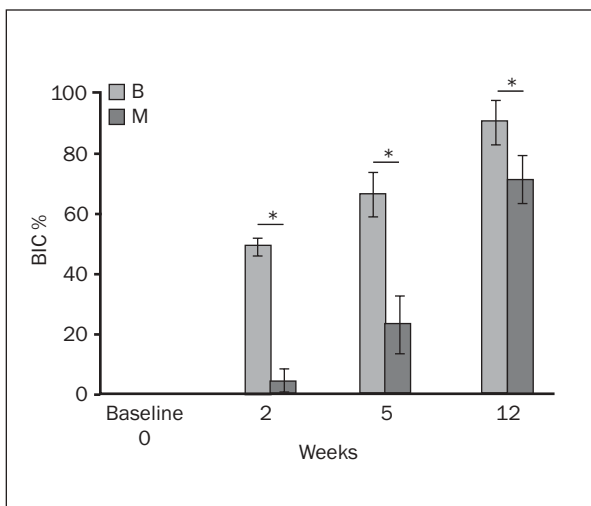
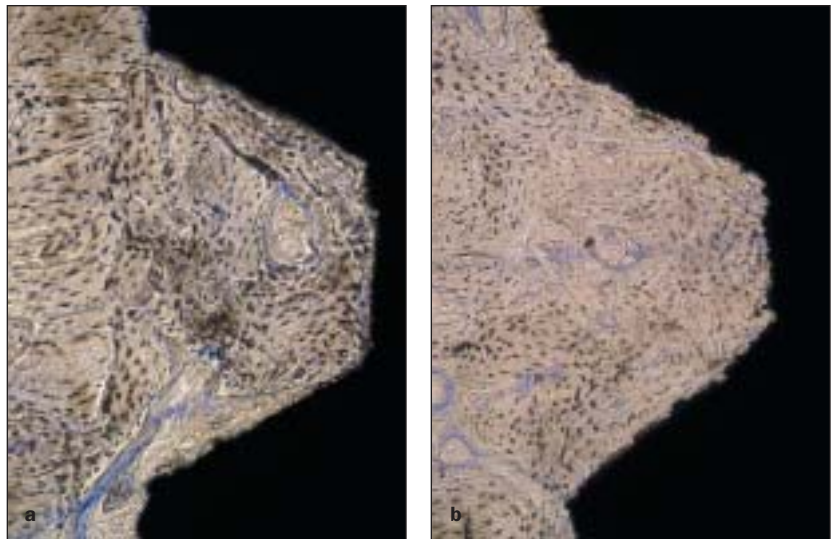


**Fig 10** Mean BIC values  $\pm$  SD for biosurfaced and machined implants at 2, 5, and 12 weeks postimplantation. \* indicates significant difference ( $P < .05$ ).

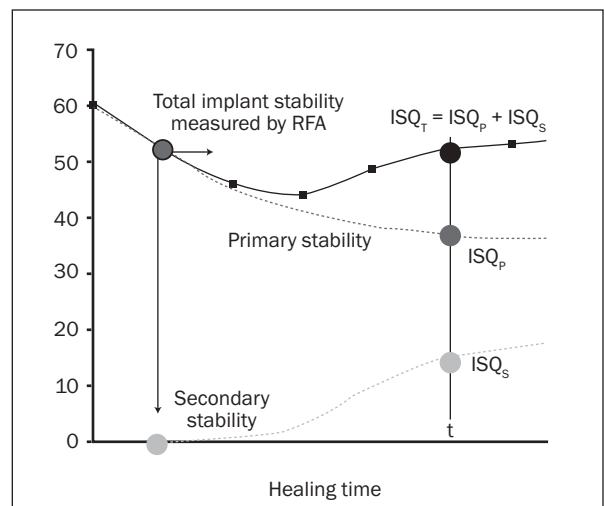


**Fig 11** Scheme of the variation in the total, primary, and secondary implant stability during healing, illustrating the relationship  $ISQ_T = ISQ_p + ISQ_s$ .

bility decreases with time as a result of mechanical bone relaxation and biologic changes associated with the original bone. Consequently, the individual data on the total stability of the implant do not provide any information on the relationship to osseointegration or the degree of BIC in the absence of information on how the secondary or primary stability contribute to the total stability value. The contribution of primary stability ( $ISQ_p$ ) must be known in order to determine that of secondary stability ( $ISQ_s = ISQ_T - ISQ_p$ ; Fig 11).

Nevertheless, in a comparative study, considering the same pattern of primary stability for the 2 types of implants compared at placement and during healing, the difference in their total implant stabilities (test  $ISQ_T - \text{control } ISQ_T$ )<sub>t</sub> measured by RFA at time point t yields the difference in the secondary stabilities according to the following formula:

$$(\text{test } ISQ_s - \text{control } ISQ_s)_t = (\text{test } ISQ_T - \text{control } ISQ_T)_t - (\text{test } ISQ_p - \text{control } ISQ_p)_t, \text{ where } (\text{test } ISQ_p - \text{control } ISQ_p)_t = 0.$$

In the animal model used, the primary implant stability (at the moment of placement) did not exhibit a statistically significant difference between the test and control groups; (test  $ISQ_p - \text{control } ISQ_p$ )<sub>t=0</sub> = 0. Furthermore, standardization of the insertion procedure and the identical shapes of the implants used for both groups of implants make it possible to assume that the variations in the primary stability with time for the test and control groups are coincident (test  $ISQ_p - \text{control } ISQ_p$ )<sub>t</sub> = 0. Under these circumstances, the stability difference (test  $ISQ_T - \text{control } ISQ_T$ ) observed experimentally from RFA measurements representing the net contribution of the biosurface to the implant stability may be considered equal to the difference in the secondary stabilities (test  $ISQ_s - \text{control } ISQ_s$ ) of implants with biosurface (test) and the turned, machined surface (control). The slope of the dependence of (test  $ISQ_T - \text{control } ISQ_T$ ) versus healing time t then corresponds to the difference in the secondary stability rates between the implants with the biosurface and the turned, machined surface

$$\frac{(\text{test } ISQ_T - \text{control } ISQ_T)}{\Delta t} = \frac{(\Delta \text{test } ISQ_s)}{\Delta t} - \frac{(\Delta \text{control } ISQ_s)}{\Delta t}$$

where  $\Delta \text{test } ISQ_s$  and  $\Delta \text{control } ISQ_s$  correspond to the changes in ISQ values and  $\Delta t$  represents the corresponding interval of the healing time of implants in bone.

If the osseointegration rate is defined as proportional to the secondary stability rate ( $\Delta ISQ/\Delta t$ ), the

difference in the osseointegration rate between the biosurfaces and turned, machined surfaces could be estimated as a mean value at 0.843 ISQ/week within the first 9 weeks of healing.

Referring to the evaluation of the correlation between the contributions of the biosurface to ISQ and BIC, it may also be concluded that the variations in the secondary stabilities of the biosurfaced implants were proportional to the changes in the BIC within the first 5 weeks of follow-up. These findings demonstrated that the biosurface enhances secondary stability compared with the turned, machined surface as a consequence of more rapid formation of BIC in the early stages of healing.

It can be speculated that the differences in the rates of osseointegration in the initial stages of healing for the biosurfaces and the machined surfaces could be related to different surface reactivity due to the different surface material properties, eg, specific surface area, surface wettability, surface contact angle, and surface hydroxylation/hydration. In general, surface reactivity, which is a common characteristic of bioactive materials,<sup>14</sup> increases with increasing specific surface area. Therefore, the 3-dimensional macro-, micro- and nano-structured biosurface which exhibits a surface area almost 100 times larger than the turned, machined surface, may significantly enhance the surface reactivity with the surrounding ions, amino acids, and proteins, which modulate the initial cellular events at the cell-material interface.<sup>53</sup>

In addition, the easily wettable hydrophilic biosurface enables establishment of good contact between the body (specifically, blood) and the rough and porous structure of the implant, and thus contributes to cellular and biomolecular migration and adhesion.<sup>54,55</sup> This biosurface, which is rich in hydroxyl groups, in contrast to the machined surface, rapidly induces adsorption of calcium and phosphate ions on contact with the ions of the blood plasma.<sup>42</sup> The calcium phosphate-rich layer promotes adsorption and concentration of proteins<sup>56,57</sup> and constitutes a suitable substrate for the first apatite structures of the bone matrix, which are synthesized by the osteogenic cells at the beginning of the formation of the new bone tissue. This mechanism can accelerate the formation of a stable bone-implant interface formed by fusion of the biologic cement-line matrix with the reactive calcium phosphate layer on the surface.

## CONCLUSIONS

The test surface (biosurface) enhances the secondary stability at an early stage of healing compared with the turned, machined surface, as a consequence of more rapid bone-implant contact formation. In contrast to the hydrophobic turned, machined surface, the biosurface, which is rich in hydroxyl groups, exhibits hydrophilic character, a low wetting angle, and high specific surface area.

## ACKNOWLEDGMENTS

The study was supported by the Grant Agency of the Ministry of Industry and Trade of the Czech Republic (project no. FT-TA/O87). Two authors (Jakub Strnad, Zdenek Strnad) are working in the research department of the Lasak, which is one of the grant funding recipients.

## REFERENCES

- Davies JE. Mechanisms of endosseous integration. *Int J Prosthodont* 1998;11:391–401.
- Søballe K, Hansen ES, B-Rasmussen H, Jørgensen PH, Bünger C. Tissue ingrowth into titanium and hydroxyapatite-coated implants during stable and unstable mechanical conditions. *J Orthop Res* 1992;10:285–299.
- Pilliar RM. Quantitative evaluation of the effect of movement at a porous coated implant-bone interface. In: Davis EJ (ed). *The Bone-Biomaterial Interface*. Toronto: University of Toronto Press, 1995:380–387.
- Brunski JE. Biomechanical factors affecting the bone-dental implant interface. *Clin Materials* 1992;3:153–201.
- Raghavendra S, Wood MC, Taylor TD. Early wound healing around endosseous implants: Review of the literature. *Int J Oral Maxillofac Implants* 2005;20:425–431.
- Hench LL. Surface reaction kinetics and adsorption of biological moieties: A mechanistic approach to tissue attachment. In: Davies JE (ed). *The Bone-Biomaterial Interface*. Toronto: University of Toronto Press, 1995:33–48.
- Cochran DL, Buser D. Bone response to sandblasted and acid-attacked titanium: Experimental and clinical studies. In: Davies JE. *Bone Engineering*. Toronto: Em Squared, 2000:391–398.
- Wennerberg A, Albrektsson T, Johansson C, Andersson B. Experimental study of turned and grit-blasted screw-shaped implants with special emphasis on effects of blasting material and surface topography. *Biomaterials* 1996;17:15–22.
- Wennerberg A, Albrektsson T, Lausmaa J. Torque and histomorphometric evaluation of c.p. titanium screws blasted with 25- and 75-micron-sized particles of Al<sub>2</sub>O<sub>3</sub>. *J Biomed Mater Res* 1996;30:251–260.
- Wennerberg A, Albrektsson T, Anderson B, Krol JJ. A histomorphometric and removal torque study of screw-shaped titanium implants with three different surface topografie. *Clin Oral Implants Res* 1995;6:24–30.
- Wennerberg A, Hallgren C, Johansson C, Danelli S. A histomorphometric evaluation of screw-shaped implants each prepared with two surface roughnesses. *Clin Oral Implants Res* 1998;9:11–19.
- Wennerberg A, Albrektsson T. Suggested guidelines for the topographic evaluation of implant surfaces. *Int J Oral Maxillofac Implants* 2000;15:331–344.
- Sul YT, Johansson C, Wennerberg A, Cho LR, Chang BS, Albrektsson T. Optimum surface properties of oxidized implants for reinforcement of osseointegration: Surface chemistry, oxide thickness, porosity, roughness, and crystal structure. *Int J Oral Maxillofac Implants* 2005;20:349–359.
- Ducheyne P, Qiu Q. Bioactive ceramics: The effect of surface reactivity on bone formation and bone cell function. *Biomaterials* 1999;20:2287–3303.
- Sul YT, Johansson C, Albrektsson T. Which surface properties enhance bone response to implants? Comparison of oxidized magnesium, TiUnite, and Osseotite implant surfaces. *Int J Prosthodont* 2006;19:319–329.
- Cordioli G, Majzoub Z, Piattelli A, Scarano A. Removal torque and histomorphometric investigation of 4 different titanium surfaces: An experimental study in the rabbit tibia. *Int J Oral Maxillofac Implants* 2000;15:668–674.
- Marinho VC, Celletti R, Bracchetti G, Petrone G, Minkin C, Piattelli A. Sandblasted and acid-etched dental implants: A histologic study in rats. *Int J Oral Maxillofac Implants* 2003;18:75–81.
- Lazzara RJ. Bone response to dual acid-etched and machined titanium implant surfaces. In: Davies JE. *Bone Engineering*. Toronto: Em squared, 2000:381–388.
- Klokkevold PR, Johnson P, Dadgostari S, Caputo A, Davies JE, Nishimura RD. Early endosseous integration enhanced by dual acid etching of titanium: A torque removal study in the rabbit. *Clin Oral Implants Res* 2001;12:350–357.
- Abrahamsson I, Berglundh T, Binder E, Lang NP, Jan Lineje J. Early bone formation adjacent to rough and turned endosseous implant surfaces. An experimental study in the dog. *Clin Oral Implants Res* 2004;15:381–392.
- Buser D, Schenk RK, Steinemann S, Fiorellini JP, Fox CH, Stich H. Influence of surface characteristics on bone integration of titanium implants. A histomorphometric study in miniature pigs. *J Biomed Mater Res* 1991;25:889–902.
- Hench LL, Wilson J (eds.). *An Introduction to Bioceramics*. Singapore: World Scientific, 1999:1–23, 41–62.
- Anderson ÖH, Larisin KH. Models for physical properties and bioactivity of phosphate opal glasses. *Glastech Ber* 1988;61:141–145.
- Strnad Z. Role of the glass phase in bioactive glass-ceramics. *Biomaterials* 1992;13:317–321.
- Koga N, Strnad J, Strnad Z, Sesták J. Thermodynamics of non-bridging oxygen in silica bio-compatible glass-ceramics: Mimetic material for the bone tissue substitution. *J Therm Anal Calorim* 2003;71:927–937.
- Sul YT. The significance of the surface properties of oxidized titanium to the bone response: Special emphasis on potential biochemical bonding of oxidized titanium implant. *Biomaterials* 2003;24:3893–3907.
- Kokubo T, Ito S, Shigematsu M, Sakka S, Yamamuro T. Fatigue and life-time of bioactive glass-ceramics A-W containing apatite and wollastonite. *J Mater Sci* 1987;22:4067–4070.
- Hench LL. Bioceramics: From concept to clinic. *J Am Ceram Soc* 1991;74:1487–1570.
- Sun L, Berndt CC, Gross KA, Kucuk A. Material fundamentals and clinical performance of plasma-sprayed hydroxyapatite coatings: A review. *J Biomed Mater Res* 2001;58:570–592.
- Clemens JAM, Klein CPAT, Vriesde RC, Rozing PM, deGroot K. Healing of large (2 mm) gaps around calcium phosphate-coated bone implants: A study in goats with a follow-up of 6 months. *J Biomed Mater Res* 1998;40:341–349.

31. Strnad Z, Strnad J, Pov'ysil C, Urban K. Effect of plasma-sprayed hydroxyapatite coating on osteoconductivity of commercially pure titanium implants. *Int J Oral Maxillofac Implants* 2000;15:483–490.
32. Liao H, Fartash B, Li J. Stability of hydroxyapatite coatings on titanium oral implants (IMZ). 2 retrieved cases. *Clin Oral Implants Res* 1997;8:68–72.
33. Rohrer MD, Sobczak RR, Prasad HS, Morris HF. Postmortem histologic evaluation of mandibular titanium and maxillary hydroxyapatite-coated implants from 1 patient. *Int J Oral Maxillofac Implants* 1999;14:579–586.
34. Block MS, Gardiner D, Kent JN, Misiek DJ, Finger IM, Guerra L. Hydroxyapatite-coated cylindrical implants in the posterior mandible: 10-year observations. *Int J Oral Maxillofac Implants* 1996;11:626–633.
35. Wheeler SL. Eight-year clinical retrospective study of titanium plasma-sprayed and hydroxyapatite-coated cylinder implants. *Int J Oral Maxillofac Implants* 1996;11:340–350.
36. Geurs NC, Jeffcoat RL, McGlumphy EA, Reddy MS, Jeffcoat MK. Influence of implant geometry and surface characteristics on progressive osseointegration. *Int J Oral Maxillofac Implants* 2002;17:811–815.
37. McGlumphy EA, Peterson LJ, Larsen PE, Jeffcoat MK. Prospective study of 429 hydroxyapatite-coated cylindrical Omniloc implants placed in 121 patients. *Int J Oral Maxillofac Implants* 2003;18:82–92.
38. Schwartz-Arad D, Mardinger O, Levin L, Kozlovsky A, Hirshberg A. Marginal bone loss pattern around hydroxyapatite-coated versus commercially pure titanium implants after up to 12 years of follow-up. *Int J Oral Maxillofac Implants* 2005;20:238–244.
39. Kim HM, Miyaji F, Kokubo T, Nishiguchi S, Nakamura T. Graded surface structure of bioactive titanium metal prepared by chemical treatment. *J Biomed Mater Res* 1999;45:100–107.
40. Ellingsen JE, Johansson CB, Wennerberg A, Holmén A. Improved retention and bone to implant contact with fluoride modified titanium implants. *Int J Oral Maxillofac Implants* 2004;19:659–666.
41. Ellingsen JE. On the properties of surface-modified titanium. In: Davies JE (ed). *Bone Engineering*. Toronto: Em Squared, 2000:183–189.
42. Strnad J, Protivinsky J, Mazur D, et al. Interaction of acid and alkali treated titanium with dynamic simulated body environment. *J Therm Anal Calorim* 2004;76:17–31.
43. Jonášová L, Müller FA, Helebrand A, Strnad J, Greil P. Biomimetic apatite formation on chemically treated titanium. *Biomaterials* 2004;25:1187–1194.
44. Strnad J, Helebrand A, Mráz R. Effect of titanium processing on the bioactivity of sodium titanate gel layer. In: Stallforth H, Revell P (eds). *Materials for Medical Engineering*. Euromat 99 (vol 2). Weinheim: Wiley-VCH, 2000:133–139.
45. Strnad J, Helebrand A. Kinetics of bone-like apatite formation in simulate body fluid. In: Helebrand A, Maryska M, Kasa S (eds). *Proceedings of the 5th ESG Conference, Glass Science and Technology for the 21st Century*. Prague: Czech Glass Society, 1999:9–16.
46. Jonášová L, Hlavác J. Effect of chemical treatment of titanium on apatite formation. In: Stallforth H, Revell P (eds). *Materials for Medical Engineering*. Euromat 99 (vol 2). Weinheim: Wiley-VCH, 2000:126–132.
47. Strnad J, Helebrand A, Hamáčková J. Bone-like apatite formation in titanium and silica glass. *Glastechn Ber* 2000;73(C1):262–269.
48. Donath K, Breuner GA. Method for the study of undecalcified bones and teeth with attached soft tissues. The Sage-Schliff (sawing and grinding) technique. *J Oral Pathol* 1982;11:318–321.
49. Rasmusson L, Kahnberg KE, Tan A. Effects of implant design and surface on bone regeneration and implant stability. *Clin Implant Dent and Relat Res* 2001;3:2–8.
50. Rasmusson L, Meredith N, Cho H, Sennerby L. The influence of simultaneous vs delayed placement on stability of titanium implants in onlay bone grafts. *Int J Oral Maxillofac Surg* 1999;28:224–231.
51. Friberg B, Sennerby L, Meredith N, Lekholm U. Comparison between cutting torque and resonance frequency measurement of maxillary implants. *Int J Oral Maxillofac Surg* 1999;28:297–303.
52. Rompen E, DaSilva D, Hockers T, et al. Influence of implant design on primary fit and stability. *Applied Osseointegration Res* 2001;2:9–11.
53. Keselowsky BG, Collard DM, Garcia AJ. Surface chemistry modulates focal adhesion composition and signalling through changes in integrin binding. *Biomaterials* 2004;25:5947–5954.
54. Lampin M, Warocquier-Cclerout R, Legris C, et al. Correlation between substratum roughness and wettability, cell adhesion and cell migration. *J Biomed Mater Res* 1997;36:99–108.
55. Webb K, Hlady V, Tresco PA. Relative importance of surface wettability and charged functional groups on NIH 3T3 fibroblast attachment, spreading, and cytoskeletal organization. *J Biomed Mater Res* 1998;41:422–442.
56. El-Ghannam A, Ducheyne P, Shapiro IM. Formation of surface reaction products on bioactive glass and their effects on the expression of the osteoblastic phenotype and the deposition of mineralized extracellular matrix. *Biomaterials* 1997;18:295–303.